Original Research Paper

JIC *Journal of Industrial Catalysis Vol. 1, No. 1, 2023, 1-8.*

Synthesis of novel DFNS/btb/Sn nanoadsorbent and its effect on color removal in industrial wastewater

Fatemeh Amarloo[1], Rahele Zhiani[1, 2*], Alireza Motavalizadehkakhky[1, 3], Malihesadat Hosseiny[1]

[1]Department of Chemistry, Neyshabur Branch, Islamic Azad University, Neyshabur, Iran.
[2]New Materials Technology and Processing Research Center, Department of Chemistry, Neyshabur Branch, Islamic Azad University, Neyshabur, Iran.
[3]Advanced Research Center for Chemistry, Biochemistry & Nanomaterial; Neyshabur Branch, Islamic Azad University, Neyshabur, Iran.
* E-mail: R_zhiani2006@yahoo.com

Received ٢٠ January 2023; accepted 1٦ May 2023

Abstract
The increase in population and the expansion of industries and technological progress are the factors that have caused an increase in water consumption and wastewater production and environmental pollution and forced investment into treatment. In this research, the color absorption capability in the presence of Sn NPs stably placed on the surface of dendritic fibrous nanosilica by 1, 3-bis (dimethylthiocarbamoyloxy) benzene (DFNS/btb/Sn) can be considered a suitable option in industries and wastewater treatment due to its physical and chemical structure. The adsorption properties of the nanocomposite were investigated. SEM, TEM, and XRD analyzes were carried out to confirm the nanoadsorbent after the confirmation of the nanoadsorbent synthesis was obtained. Its industrial application was investigated in the removal of dye from the textile factory effluent. Reactive red dye 198 was removed from textile wastewater and the best removal efficiencies of 93, 92.2, and 90.5 percent were obtained for the initial dye concentration of 20, 40, and 60 mg/L, respectively, at optimal pH=5 and reaction time of 45 minutes. To determine the type of adsorption isotherm, Langmuir, Nernst and Freundlich adsorption isotherms were used by DFNS/btb/Sn nanoadsorbent, and the results show that the adsorption behavior follows the Langmuir adsorption isotherm equation. In addition, the recyclability of DFNS/btb/Sn was easily separated from the solution and reused ten times. This research can be used as an effective option for the final treatment of wastewater containing low to medium concentrations of dyes.
Keywords: *Wastewater, Nanoparticle, Adsorbent, Dye*

1. Introduction
Scientists are looking the development of a unique method for sewage treatment, which improves the quality of the sewage output more than the existing methods without using expensive chemicals. Wastewater treatment, with the help of nano-adsorbent, can simultaneously remove organic and mineral compounds and turn wastewater into a suitable water source. It will lead to a decrease in the penetration of sunlight, interference in the ecology of receiving waters and a decrease in the intensity of photosynthesis of aquatic plants and algae [1]. Many of the azo dyes and their broken products are toxic and carcinogenic and can lead to bladder cancer in humans. Nuclear abnormalities in tumors, allergies in laboratory animals and chromosomal mutations in mammalian cells have been proven them [2]. Due to the formation of stable complexes, the dyes are hard to decompose biologically, and frequent wastewater treatment processes are not useful for its efficient use due to low efficiency, chemical sludge production, and high cost is not considered [3]. Various methods such as coagulation and coagulation, chemical oxidation, electrochemical filtration, and surface absorption process have been studied for textile industry wastewater treatment [4-8]. Recently, advanced oxidation processes have been widely considered as alternatives to conventional processes. In advanced oxidation processes, hydroxyl radical (OH) is produced as the main factor of the oxidation of organic compounds in the environment. This radical is very reactive and, due to the presence of an unpaired electron, it can non-selectively oxidize organic compounds [9]. Nowadays, the photocatalytic decomposition of color solutions has a special place in industrial applications due to the possibility of making efficient nano photocatalyst, Ezran, high efficiency of decomposition and high speed of photocatalytic reaction [10]. There are several technologies in the framework of physical, chemical and biological processes for the treatment of different types of wastewater. Although it is clear that many of these conventional technologies have limitations from an economic point of view. It is expected that the use of new forms of low-cost absorbent materials has the potential to achieve this goal [11]. Wastewater treatment using the absorption method has provided a very suitable topic for research in this field. Low-cost absorbents have been proposed for various types of toxic chemicals in wastewater. The existing and developed materials can be modified to increase the capacity or activity by several methods, which causes more efficiency in their applications. Due to their high surface area and porosity, nanoparticles are a good example of purifying almost all available pollutants [12-18]. The set of metals has strong catalytic behavior. Many studies have been done in this

field, and metals used in the analysis is known as the most stable catalyst with analytical properties that can be used in various applications such as Sonogashira, Heck, Suzuki-Miyaura, pollutant degradation, Hiyama, Larocque heterovalence, fuel cells and hydrogenation, recently, it has been proven [19-23]. Which, in terms of inhibiting the accumulation of metal catalysts, the use of complex functional groups, both on the solid edges impregnated or grafted, plays a significant role. Metal-organic frameworks (MOFs) have been widely investigated by researchers because they can provide many applications in the field of gas analysis, separation and storage, as well as O2 absorption. Heterogeneous analysis by small metal nanoparticles or MOF nanocomposites supported by nanoparticles or nanocomposites (NCs) is a very important field in science because it is possible to use MOF nanocomposites as templates for producing metal NPs/NCs and representing microenvironments. Be used clearly, which can induce selective control in NPs/NCs [24-29]. First, chemical vapor deposition is carried out by depositing metal in MOF in the gas phase, using organometallic precursors [30-37]. In the study of Asgari et al., to investigate the effect of changes in pH, time, and different concentrations of titanium dioxide on the efficiency of the process, 100 ml of wastewater sample was placed inside the reactor along with titanium dioxide, and then the amount of the remaining color was read. The results of color removal at pH=7, duration of 120 minutes and concentration of 1 g/l of TiO2 with 80.523% and its COD with 64.75% efficiency were obtained [38]. The results of Mozafari et al.'s experiment showed the highest color removal efficiency at a pH=3. The highest removal rate was obtained in the first 60 minutes of the experiment. As the initial dye concentration increased, the removal efficiency decreased. The obtained results showed that by increasing the amount of adsorbent from 0.4 to 0.8 g per 100 ml, the removal efficiency does not change much, so for the concentrations of 25 and 50 mg/l, the removal efficiency is 12.00, respectively. 93% has increased to 95.41% and from 90.83% to 93.96%. The dye absorption isotherm using reed plant powder follows the Longmire isotherm model [39]. The purpose of this study of wastewater treatment is to reduce the pollutants in it so that it does not pose a threat to human health or the environment.

2- Experimental method

2-1-Laboratory tools used

High-purity chemicals were purchased from Fluka and Merck. Melting points were determined using an Electrothermal 9100 device. Particle size and structure of nanoparticles were observed using a Philips CM10 transmission electron microscope at a speed of 100 kV. Field emission scanning electron microscopy (FE-SEM) images were acquired on a HITACHI S-4160. XPS studies were performed using an XR3E2 twin anode X-ray source (VG Microtech) with AlKα = 1486.6 eV. Powder X-ray diffraction data were obtained using a Bruker D8 Advance model with Cu ka emission. ICP experiments were performed using a simultaneous ICP-OES VARIAN VISTA-PRO CCD instrument. The surface area, pore volume and pore diameter of the obtained NPs were determined by N2 adsorption at -196 ℃ with a surface and pore size analysis (Micromeritics ASAP 2000 instrument) using the BET method. Determining the purity of the products and monitoring the reaction was done by TLC on polygram silica gel plates SILG / UV 254. Magnetic stirrer heater stirrer made by IKA company in England, Universal laboratory oven model UF110 product by Memmert company made in Germany, electronic balance laboratory scale model 2K001, laboratory centrifuge model CENTRIC MF 48 made by Domel were used.

2-2- Sampling

A sampling of the wastewater of the Mashhad textile factory was done in several time frames and taking into account the basic parameters including physical and chemical conditions, pH and temperature of the wastewater.

The sample of reactive red azo dye 198 studied with its molecular weight 556.49, 509 nm and its chemical formula (C22H14N4Na2O7S2) was obtained from the textile company. H2SO4 and NaOH for pH adjustment, $AlCl_3$, Na2CO3, Mg $(CH_3COO)_2$, NaOH, HCl, MgCl2.6H2O, and ethanol were purchased from Merck.

2-3-DFNS synthesis method

Tetraethyl orthosilicate (TEOS) (3.5 g) was dissolved in a solution of cyclohexane (40 ml) and 1-pentanol (3.0 ml). Then, a mixed solution of acetylpyridinium bromide (CPB) (1.5 g) and urea (0.9 g) was dissolved in H2O (45 ml) and stirred continuously for 45 min at room temperature. Then it was placed in a hydrothermal reactor with Teflon and heated at 130°C for 3 h. The produced silica was centrifuged, washed with a mixture of deionized water and acetone and dried in an oven. The product was calcined at 600°C for 6 h [40].

2-4- DFNS/btb NPs synthesis method

DFNS (1 g), 50 ml of DMF, and 1.5 mmol of 3, 5-dihydroxybenzoic acid were mixed. The reaction mixture was stirred for 35 h, under a temperature of 110℃. Then filtered and washed by DMF and finally dried in an oven at 80°C for 24 h to produce DFNS/btb NPs. After that, one gram of the obtained solid, 5.5 g of potassium carbonate (K2CO3), and 5 g of, N, N-dimethylthiocarbamoyl chloride were stirred in 100 ml of acetone and refluxed in the presence of nitrogen for 45 h. After cooling the suspension, the solvent was removed under a vacuum. After that, the separated organic phase was washed with deionized water, KOH (7%), and saturated NaCl and finally dried over Na2SO4 [41].

2-5-Preparation method for obtaining DFNS/btb/Sn NPs:

To obtain DFNS/btb/Sn, we first mix DFNS/btb (1 g) with 1 mmol Sn (OAc) 2. Then it was placed by 20 ml of CH2Cl2 at 25°C for 24 h. And finally, the filtrate mixture was washed with acetonitrile [41].

The production of DFNS/btb/Sn nano adsorbent includes many steps. On DFNS surfaces, it contains many N-H groups. Therefore, it is predicted that DFNS can be simply utilized by 1, 3-bis (dimethylthiocarbamoyloxy) benzene to form DFNS/bpt. In addition, 1, 3-bis (dimethylthiocarbamoyloxy) benzene groups can support Sn (II) complexes over DFNS/btb (Figure 1).

2-6-pH measurement

To read the pH, the water that was just sampled was poured into a completely clean cup and the sample was placed under the pH meter device and the pH of the water was measured. Also, before the reading, the device was calibrated by the available buffers. Continue the pH measurement until the number is fixed so that the number read is the same in at least two consecutive repetitions. We took the constant read number as the pH of the sample and noted it down. Note: If the number read for the pH of the sample is different in consecutive repetitions, this process should be continued until the number read in 3 consecutive repetitions are very close to each other, in this case, it is possible to average between three consecutive similar readings and the average number reported as the pH of the sample.

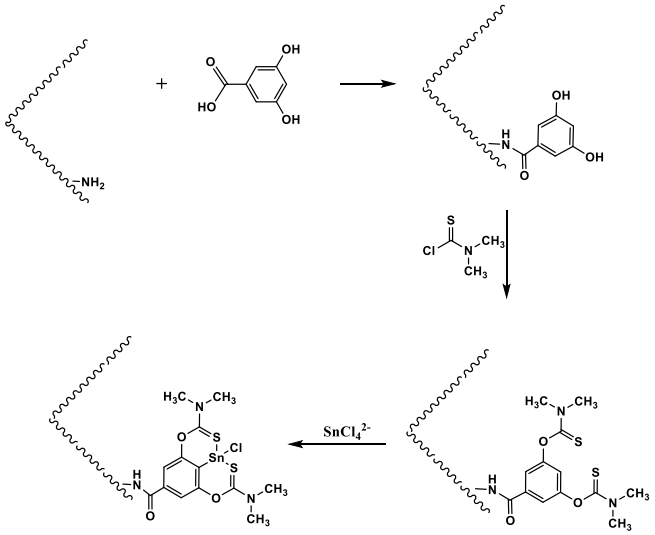

Figure 1- Synthesized schematic image for DFNS/btb/Sn (II)

2-7- color measurement

To measure the color at the end of each test, 10 mL samples were taken and centrifuged for 5 min at 4400 rpm to separate the adsorbent. The color concentration was measured using a DR5000 spectrophotometer at the maximum absorption wavelength of 509 nm in the visible range. The temperature was measured with a thermometer and pH with a Cyberscan digital pH meter. All the laboratory data presented during the studies were based on the arithmetic mean, with at least 3 repetitions of the experiment, which were recorded after removing the distorted and wrong data. A 3-Mira XMU field emission electron microscope was used to examine the surface structure of the produced adsorbent.

The pH of the zero electric charge point (pHzpc) of nanoparticles was determined by mixing 0.2g of nanoparticles with 50 ml of NaCl (0.01 M) red standard solution in 10 separate Erlenmeyer flasks. Add the required amounts of HCl or NaOH to each Erlenmeyer to set pH= 2.5, 3, 4, 5, 6, 7, 8, 9, 10 and 11. The mixture was stirred for 24 h at ambient temperature at 120 rpm and then the equilibrium pH was measured. The value of pHzpc will be equivalent to the pH in which the primary and secondary pH values are the same after mixing for 24 hours [42].

3- Results

3-1- TEM and SEM examination of nanoparticles

The morphology and sizes of DFNS/btb/Sn(II) nanoadsorbent were determined using SEM and TEM. Nanoparticles have been synthesized uniformly. They also have the same surface and the average diameter of the microspheres is around 100-120 nm (see Figure 2).

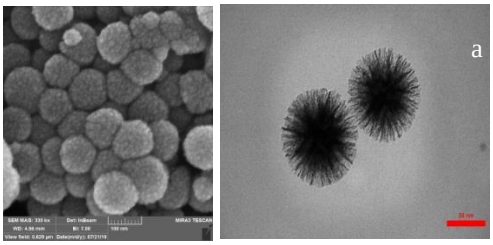

Figure 2. Images from DFNS/btb/Sn (II) (a) SEM, (b) TEM

3-2- Examination of X-ray diffraction (XRD) of DFNS/btb/Sn (II) nanoparticles

Figure 3 shows the X-ray diffraction patterns of DFNS and DFNS/btb/Sn, respectively. The XRD pattern of the generated DFNS pattern (Figure 3a) is amorphous. Figure 3b shows a common XRD curve for DFNS/btb/Sn NPs.

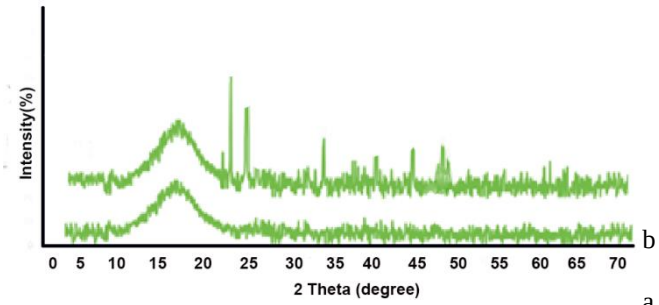

Figure 3 XRD analysis: (a) DFNS; (b) DFNS/btb/Sn.

3-3- Thermometric analysis (TGA)

This is done at different temperatures to verify the thermal stability of DFNS/btb/Sn, as seen in Figure 4. There are two stages of weight loss. Regarding the loss of small molecules such as physically adsorbed water, about 4% weight loss is seen in the first stage under the temperature range of 40 to 250°C. In the second stage, the temperature is in the range of 250 to 400℃, and the

weight is reduced by about 72%, which may be due to the derivatives of the organic group.

3-4-absorption-desorption isotherms

The specific porosity and surface area of the supported adsorbent, fresh adsorbent, and recycled adsorbent, as well as the initial MOF are obtained using the Barrett-Joyner-Holland (BJH) and Brunner-Emmett-Teller (BET) theory.

The N2 adsorption and desorption isotherms of DFNS /btb/Sn nanoparticles show a type IV curve that is consistent with previous studies on standard porous materials (Figure 5).

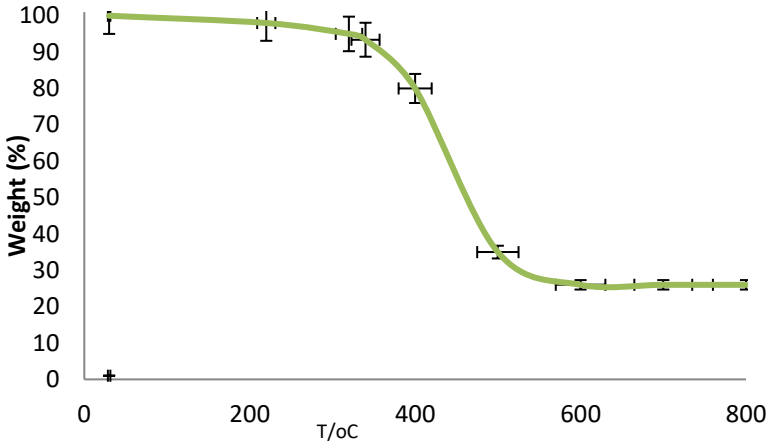

Figure 4 - TGA diagram of DFNS/btb/Sn

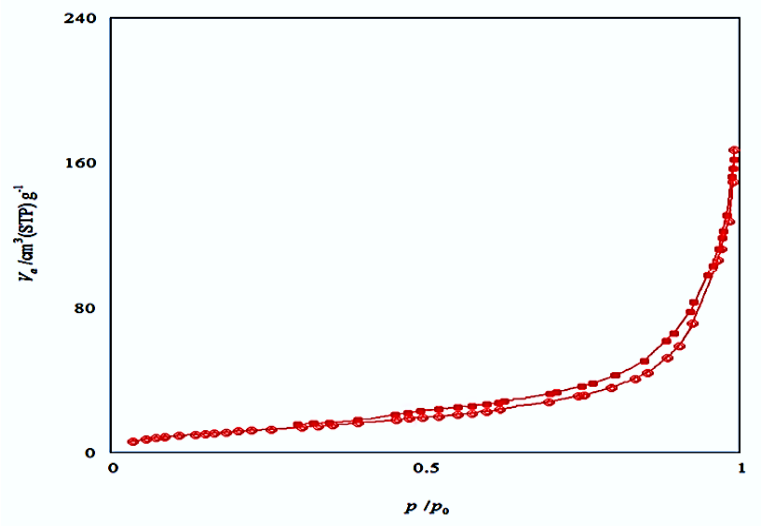

Figure 5- Absorption-desorption isotherms of DFNS/btb/Sn.

As can be seen in Table 1, after the synthesis of DFNS/btb/Sn and the addition of btb/Sn on the surface of DFNS nanoparticles, the desired surface porosity has decreased. The surface of the adsorbent has been significantly reduced, which is the formation of btb/Sn after synthesis on the surface.

Table 1- Structural elements of DFNS/btb/Sn and DFNS materials determined from the nitrogen absorption test.

Adsorbents	S_{BET} (m^2 g^{-1})	V_t (cm^3 g^{-1})	D_{BJH} (nm)
DFNS	1274	0.549	1.82
DFNS / btb / Sn	932.6	0.410	2.41

3-5-Investigating the color removal parameters of industrial wastewater

Colored compounds and mainly azo dyes in the effluents of various industries, such as textile industries, are among the biggest environmental pollutants with health hazards that are resistant to biological treatment. The efficiency of nanoparticles was determined in the treatment of textile wastewater, where reactive azo dye 198 was used as a model pollutant.

3-5-1- pH effect

The effect of pH was studied in the range of 3-9, at a fixed concentration of nanoparticles of 0.5 g/L, the ambient temperature of 24±3 ℃ and mixing speed of 250 rpm in a reaction time of 60 min. The color removal efficiency decreased in parallel with the increase in pH. The highest color removal efficiency of 67.7 and 61.2% was observed at pH=3 and 5 (Figure 6).

The pHzpc of the nanoadsorbent was equal to 8.3. Considering the non-significance of color yield difference ($p<0.05$) and pH=5 was chosen as the best value.

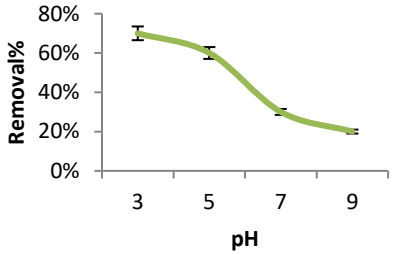

Figure 6- The effect of pH on the efficiency of the catalytic decomposition process based on nanoparticles in the removal of reactive red dye 198 (reaction time 60 min, initial dye concentration 20 mg/L, adsorbent 0.5 g/L)

3-5-2-Effect of the amount of nanophotocatalyst

The optimization of nanoparticles in the range of 0.2 to 1.5 g/L was studied at a pH =5 and a reaction time of 60 minutes. The removal efficiency increased in parallel with the increase in the amount of nanoparticles up to a concentration of 0.8 g/L, and after that, no significant effect was observed (Figure 7). The color removal efficiency of nanoparticles was equal to 0.8 g/L, equivalent to 92.2%.

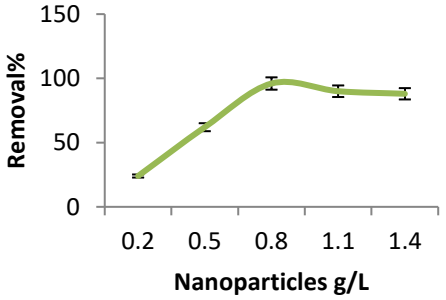

Figure 7- The effect of DFNS/btb/Sn nanoparticle concentration on the efficiency of the adsorbent decomposition process in the removal of reactive red dye 198

3-5-3-Effect of reaction time

The effect of reaction time in the range of 15 to 60 min at a concentration equal to 0.8 g/L, pH=5, UVA radiation on the yield of reactive red 198 dye was studied (Figure 8). In parallel with the increase in time, the removal efficiency has increased. The color removal efficiency was 91.9 and 92% at reaction times of 15, 30, 45 and 60 min, respectively. Due to the lack of significant difference between the removal efficiency values of 45 and 60 min reaction times, 45 minutes reaction time was chosen as the optimal level.

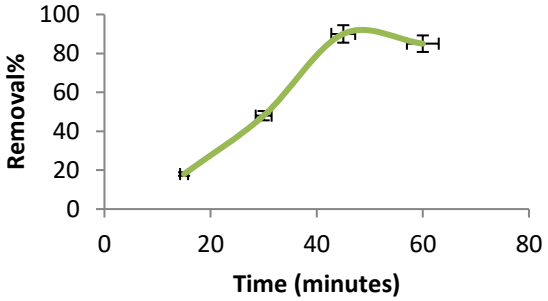

Figure 8- The effect of contact time on the efficiency of the catalytic decomposition process in the removal of reactive red dye 198

3-5-4-Effect of initial color concentration

The effect of the initial concentration of the dye on the optimal levels of other variables, including pH=5, the concentration of nanoparticles 0.8 g/L, and reaction time of 45 min, was studied. Increasing the initial concentration of the dye up to the initial concentration of 60 mg/L did not have much effect on reducing the dye efficiency, but at higher concentrations, the dye removal efficiency had a noticeable decrease. The color removal efficiency was 93, 92.2, 90.5, 82 and 74.7% for initial concentrations of 20, 40, 60, 80 and 100 mg/L, respectively (Figure 9).

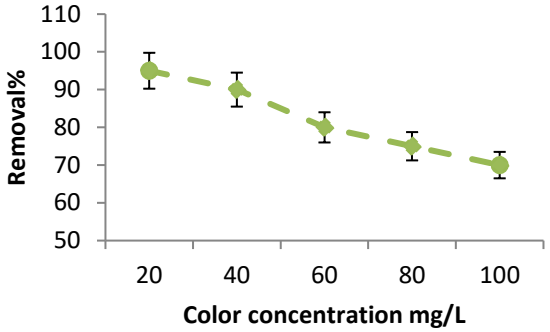

Figure 9- The effect of the initial dye concentration on the efficiency of the adsorbent decomposition process in the removal of reactive red dye 198

3-5-5- Langmuir adsorption isotherm

This isotherm is used in the case where the number of absorption positions in the adsorbent is limited and only one molecule is absorbed at each absorption position. Based on this theory, a specific amount of the substance can be absorbed and, after reaching the saturation point (a point after which there is no possibility of absorption), the increase of the absorbed substance will not increase the absorption. Langmuir adsorption isotherm relation can be shown as equation 1.

$$qe=QbCe/ (1+bCe) \qquad \text{Equation 1}$$

$$1/qe=1/Q=1/QbCe$$

In this relationship, Q (mg/g) is the maximum amount of absorbed dye per unit of adsorbent weight, Ce (mg/l) is the dye concentration in the bath at the equilibrium point, qe (mg/g) is the amount of absorbed dye per gram. Calder is the equilibrium point and b (ml/mg) is the Langmuir constant, which is related to the tendency of absorption in adsorbent materials.

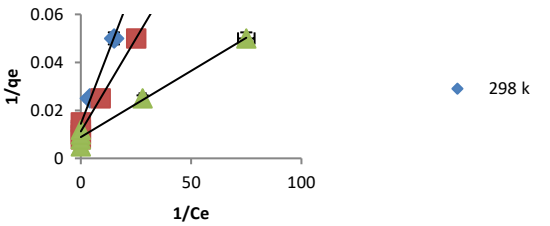

Figure 10. Langmuir adsorption isotherm for the adsorption of reactive dye red 198 by DFNS/btb/Sn

Nano DFNS/btb/Sn Figure 11 shows the graph of 1/qe versus 1/Ce for the absorption of 198 red reactive dye on nano DFNS/btb/Sn. The values of Q and b, respectively, the width from the origin and the angle coefficient of the lines obtained for different temperatures are calculated and presented in Table 2. The results show that the convergence coefficients obtained for different lines (different temperatures) are more consistent with the Langmuir adsorption isotherm (R2<0.95). These results show that increasing the temperature increases the values of Q and b. The increase in Q with the increase in temperature is proof of the absorption process being endothermic. Also, the increase of b with increasing temperature shows that the highest value of adsorption affinity is at the highest temperature.

Table 2- Different parameters of the Longmire adsorption isotherm for the adsorption of Reactive Red 19 by DFNS/btb/Sn

T(K)	B(L/mg)	Q(mg/g)	R^2
298	2.178	102.041	**0.9732**
308	3.760	106.383	**0.9787**
318	15.167	109.890	**0.981**

3-5-6-Freundlich adsorption isotherm

Another important adsorption isotherm that is important in the study of dye adsorption behavior with adsorbent is the Freundlich adsorption isotherm. This type of isotherm is true for dye adsorption in unlimited situations. This type of adsorption isotherm is used for surfaces with heterogeneous surface energy. In this adsorption isotherm, the dye absorption increases rapidly with the increase of the initial concentration of the dye, and after occupying a significant number of absorption positions in the adsorbent, the absorption rate decreases. The Freundlich adsorption isotherm equation is in the form of equation 2 below.

$$qe=QfCe1/n \qquad \text{Equation 2}$$

Where Q (mg/g) is the maximum amount of dye absorbed per unit weight of the absorbent and 1/n indicates the absorption intensity. The linear relationship of this isotherm is also in the form of equation 3.

$$lnqe=lnQf+1/nlnCe \qquad \text{Equation 3}$$

The values of Qf and 1/n are obtained by plotting Inqe versus InCe.

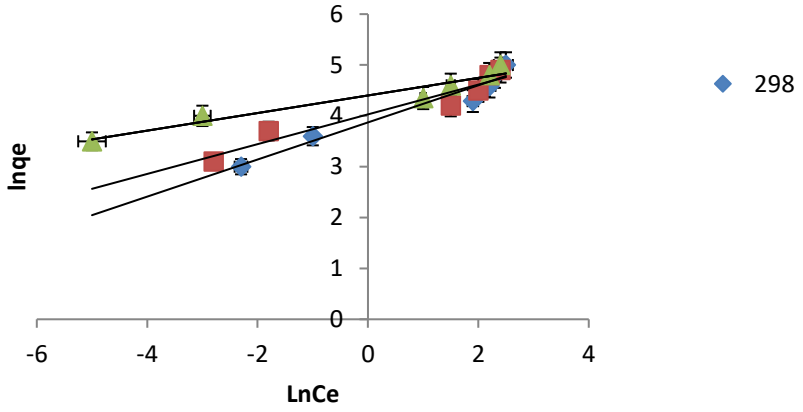

Figure 11. Freundlich adsorption isotherm for the adsorption of reactive dye 198 red by DFNS/btb/Sn

The Freundlich adsorption isotherm results are presented in Figure 11 and Table 3. The results show that the values increase with increasing temperature, and this is due to the absorption process being endothermic. Also, n being larger than 1 indicates the suitable conditions for reactive dye absorption by DFNS/btb/Sn nanoparticles. Further, by examining the convergence coefficients of the obtained lines, it can be seen that this isotherm can also be used to check the absorption of dyes by the adsorbent, but according to the convergence coefficients, it is more consistent with the Langmuir adsorption isotherm.

Table 3- Different parameters of Freundlich adsorption isotherm for adsorption of reactive dye red 198 by DFNS /btb/Sn

T(K)	Qf(mg/g)	N	R^2
298	49.368	2.652	**0.9507**
308	59.199	2.916	**0.9247**
318	78.023	3.549	**0.9325**

3-5-7-Nernst adsorption isotherm

The Nernst adsorption isotherm equation 4 is as follows.

qe=kfCe Equation 4

In this regard, qe (mg/g) is the amount of dye absorbed per gram of goods at the equilibrium point, Ce (mg/L) is the dye concentration in the bathroom at the highest equilibrium point (objects), and Kf (mg/g) is the maximum amount. The absorbed color is per unit weight of the absorbent.

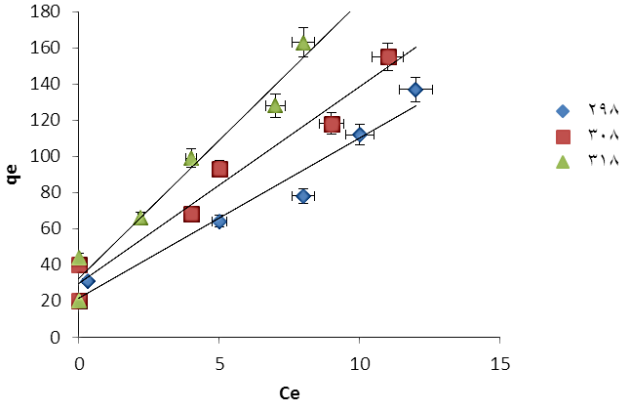

Figure 12 – Nernst adsorption isotherm for the adsorption of reactive dye red 198 by DFNS/btb/Sn

Figure 12 and Table 4 show that the values increase with increasing temperature and this is due to the endothermic nature of the absorption process. Also, the Nernst absorption isotherm is weaker to describe the behavior of reactive red 198 absorptions by nanoparticles.

Table 4- Different parameters of Nernst adsorption isotherm for adsorption of reactive dye red 198 by DFNS/btb/Sn nanoparticles

T(K)	K_f (mg/g)	R^2
298	10.296	**0.9663**
308	12.587	**0.9657**
318	16.824	**0.9641**

4-Conclusion

Metal-organic frameworks are coordination polymer compounds that are composed of metal as nodes and organic ligands as linkers. These compounds are crystalline and porous, and the size and shape of their holes can be engineered. These features, along with a very high surface-to-volume ratio, have made them useful for various applications, such as heterogeneous adsorbents, absorbents, gas separation, and storage

agents, sensors, fuel cells, solar cells, and the removal of environmental pollutants. In addition to the easy synthesis method, convenient recyclability and recovery, it is concluded that DFNS/btb/Sn can be stable and degraded in the removal and degradation of pharmaceutical organic pollutants. According to the results of dye removal from textile wastewater, it can be concluded that nanoparticles have a suitable capability as an adsorbent and the high efficiency of reactive red 198 dye removal indicates that the studied process can be an effective option for the final treatment of wastewater. Contains low to medium concentrations of colored compounds.

References

[1] E. H. Ezechi, S. Kutty, A. Malakahmad, M. H. Isa, Process Saf. Environ. Prot. 98 (2015) 16.
[2] A. Almasian, M. E. Olya, N. M. Mahmoodi, J. Taiwan Inst. Chem. Eng. 49 (2015) 119.
[3] S. An, X. Liu, L. Yang, L. Zhang, Chem. Eng. Res. Des. 94 (2015) 726.
[4] L. Kernazhitsky, V. Shymanovska, T. Gavrilko, V. Naumov, L. Fedorenko, V. Kshnyakin, J. Baran, J. Lumin. 166 (2015) 253.
[5] K. B. Tan, M. Vakili, B. A. Horri, P. E. Poh, A. Z. Adullah, B. Salamatinia, Sep. Purif. Technol. 150 (2015) 229.
[6] M. M. Haque, W. T. Smith, D. K. Y. Wong, J. Hazard. Mater. 83 (2015) 164.
[7] C. Z. Liang, S. P. Sun, F. Y. Li, Y. K. Ong, T. S. Chung, J. Membr. Sci. 469 (2014) 306.
[8] Y. Wei, A. Ding, L. Dong, Y. Tang, F. Yu, X. Dong, Colloids Surf., A Physicochem. Eng. Asp. 470 (2015) 137.
[9] V. V. Ranade, V. M. Bhandari, Butterworth-Heinemann (2014).
[10] J. Zhang, G. Chen, M. Chaker, F. Rosei, D. Ma, Appl. Catal. B: Environ. 132 (2013) 107.
[11] F. Cardenas-Lizana, D. Lamey, N. Perret, S. Gomez-Quero, L. Kiwi-Minsker, M. A. Keane, Catal. Commun. 21 (2012) 46.
[12] S. E. Baghbamidi, A. Hassankhani, E. Sanchool, S. M. Sadeghzadeh. Appl. Organomet. Chem. 32 (2018) 4251.
[13] S. M. Saadati, S. M. Sadeghzadeh. Catal. Lett. 148 (2018) 1692.
[14] K. Sumida, D. L. Rogow, J. A. Mason, T. M. McDonald, E. D. Bloch, Z. R. Herm, T. H. Bae, J. R. Long, Chem. Rev. 112 (2012) 724.
[15] S. M. Sadeghzadeh, R. Zhiani, S. Emrani, Catal. Lett. 148 (2018) 119.
[16] M. Yoosefian, A. Mola, E. Fooladi, S. Ahmadzadeh, J. Mol. Liq. 225 (2017) 34.
[17] N. Etminan, M. Yoosefian, H. Raissi, M. Hakimi, J. Mol. Liq. 214 (2016) 313.
[18] M. Yoosefian, Appl. Surf. Sci. 392 (2017) 225.
[19] S. M. Sadeghzadeh, J. Mol. Liq. 223 (2016) 267.
[20] X. Le, Z. Dong, X. Li, W. Zhang, M. Le, J. Ma, Catal. Commun. 59 (2015) 21.
[21] O. A. O'Connor, L. Y. Young, Environ. Toxicol. Chem. 8 (1989) 853.
[22] R. Zhiani, J. Chem. Res. 41(2017) 425.
[23] K. Li, Z. Zheng, X. Huang, G. Zhao, J. Feng, J. Zhang, J. Hazard. Mater. 166 (2009) 213.
[24] Y. Zhang, X. Yuan, Y. Wang, Y. Chen, J. Mater. Chem. 22 (2012) 7245.
[25] S. Saha, A. Pal, S. Kundu, S. Basu, T. Pal, Langmuir 26 (2010) 2885.
[26] Y. Yang, Y. Guo, F. Liu, X. Yuan, Y. Guo, S. Zhang, W. Guo, M. Huo, Appl. Catal. B: Environ. 142-143 (2013) 828.
[27] M. M. Mohamed, M. S. Al-Sharif, Appl. Catal. B: Environ. 142-143 (2013) 432.
[28] M. Muniz-Miranda, Appl. Catal. B: Environ. 146 (2014) 147.
[29] J. R. Li, J. Sculley, H. C. Zhou, J. Chem. Rev. 112 (2012) 869.
[30] M. P. Suh, H. J. Park, T. K. Prasad, D. W. Lim, J. Chem. Rev. 112 (2012) 782.
[31] S. M. Sadeghzadeh, R. Zhiani, M. Moradi, ChemistrySelect 3 (2018) 3516.
[32] S. M. Sadeghzadeh, ChemPlusChem 79 (2014) 278.
[33] J. L. Wang, C. Wang, W. Lin, ACS Catal. 2 (2012) 2630.
[34] Y. E. Cheon, M. P. Suh, Eur. J. Chem. 14 (2008) 3961.
[35] F. Zhang, S. Zheng, Q. Xiao, Y. Zhong, W. Zhu, A. Lin, M. S. El-Shall, Green Chem. 18 (2016) 2900.
[36] Z. Dong, X. Le, C. Dong, W. Zhang, X. Li, J. Ma, Appl. Catal. B: Environ. 162 (2015) 372.
[37] X. Cui, W. Zuo, M. Tian, Z. Dong, J. Ma, J. Mol, J. Mol. Catal. A: Chem. 423 (2016) 386.
[38] G. Asgari, A. Seidmohammadi, M. Bagheri, S. Chavoshi, UMSHA. 2 (2017) 143.
[39] S. Mozafari, M. Taghighaneian, M. Dehvari, B. Jamshidi, J. Ilam Uni. Med. Sci. 7 (2015) 119.
[40] R. Zhiani, A. Es-haghi, F. Shamsa, F. Amarloo, M. Shahroudi, Silicon. 12 (2020) 2005.
[41] Z. Kiani, R. Zhiani, S. Khosroyar, A. Motavalizadehkakhky, Hosseiny M. Inorg. Chem. Commun. 124 (2021) 108382.
[42] F. R. Furlan, L. G. de Melo da Silva, A. F. Morgado, A. A. Ulson de Souza, S. M. A. Guelli Ulson de Souza, Resour. Conserv. Recycl. 54 (2010) 283.